The study on the effect of Tellurium (Te) on the electronic structure of Iron Selenium (FeSe)

By Rajif Mulatu

A thesis submitted to the department of Applied Physics, school of Applied Natural Science

Presented in partial fulfillment of the requirements for the degree of Master of Science in Physics (Material Physics)

OFFICE OF GRADUATE STUDIES, ADAMA SCIENCE AND TECHNOLOGY UNIVERSITY

ADAMA, ETHIOPIA

JUNE 2019

The study on the effect of Tellurium (Te) on the electronic structure of Iron Selenium (FeSe)

By Rajif Mulatu

Adviser: Mesfin Asfaw(PhD)

A thesis submitted to the department of Applied Physics, school of Applied Natural Science

Presented in partial fulfillment of the requirements for the degree of Master of Science in Physics (Material Physics)

OFFICE OF GRADUATE STUDIES, ADAMA SCIENCE AND TECHNOLOGY UNIVERSITY

ADAMA, ETHIOPIA

JUNE 2019

Declaration

I hereby declare that this is my original work and has not been presented for a degree in any other university, and all sources of material used for this thesis have been duly acknowledged.

Name: Rajif Mulatu

Signature:_____

This MSc thesis has been submitted for examination with my approval as thesis adviser.

Name: Mesfin Asfaw(PhD)

Signature:----------

Date of submission _____

ADAMA SCIENCE AND TECHNOLOGY UNIVERSITY DEAPRMENT OF APPLIED PHYSICS

The undersigned hereby certify that they have read and recommend to the school of Applied Science for acceptance a thesis entitled "The study on the effect of Tellurium (Te) on the electronic structure of Iron Selenium (FeSe) "

by Rajif Mulatu Master of Science.

Dated: June 2019

Supervisor:_____

Acknowledgment

I would like to thank my adviser Dr. Mesfin Asfaw and Adama Science and Technology University, School of Applied Natural Science, department of Applied Physics. Furthermore I would like to thank my class mat and my family for their unreserved support.

Rajif Mulatu

Adama Science and Technology University

Adama, Ethiopia

TABLE OF CONTENT

List of Figure

Abstract

In this work we present the effect of tellurium (Te) on band structure, DOS and superconductivity of FeSe(for x=0.25 and x=0.5). The electronic structure calculations are performed using the density functional theory (DFT) as implemented in QUANTUM ESPRESSO (QE). All calculations of $FeSe_{1-x}Te_x$ were done for the space group P4/nmm with non-spin polarized orbitals with lattice parameters a=b=3.765[a.u], c=5.51[a.u]. We reproduced the known band structure for FeSe and FeTe. Based on the carefully prepared input file we produced the band structure for x=0.25 and x=0.5. The band structures are highly affected at x=0.5. We observed that there is a flat band from M to Γ direction. We calculated the DOS at the Fermi level to be $3.84\ states/(eV.cell)$ for $FeSe_{0.5}Te_{0.5}$ which is higher than that of FeSe which was reported to be 2.69 $states/(eV.cell)$. The $FeSe_{0.75}Te_{0.25}$ shows no superconductivity. Superconducting critical temperature T_C for $FeSe_{0.5}Te_{0.5}$ was calculated by introducing our DOS result in to the McMillan equation. The result showed that the T_C is increased to 12.08K. We concluded that the effect of substituting Te in FeSe increases the DOS and T_C. The results are in agreement with the experimental reports. We also predict that Te substitution is hole dopping.

Keywords: superconductivity (SC), band structure, density of states (DOS), and critical temperature (T_C).

Chapter 1

Introduction

1.1 Background

Superconductivity has been an exciting, fascinating and challenging topic since its discovery in 1911. Thousands of materials have been found to exhibit this phenomenon in the temperature range of a few mK to 164 K. Besides pure elements, almost all categories of materials seem to show superconductivity, including metallic alloys, intermetallics, metallic glasses, ceramics, inorganic and organic polymers and various forms of carbon like fullerenes. Over the last 10 decades, the field has proved itself to be extraordinarily rich and dynamic with new discoveries, in the form of a novel material or phenomenon.

Superconductivity was observed for the first time by a Dutch physicist Heike Kamerlingh Onnes, a professor of physics at the University of Leiden. He successfully liquefied Helium in 1908 and was subsequently able to reduce the temperature of liquid helium (LHe) down to as low as 0.9K. He had intended to measure the resistivity of metals as a function of temperature at very low temperatures. By measuring the resistivity of mercury (Hg), as a high purity metal, he found in 1911 that the electrical resistivity of Mercury abruptly dropped to zero, when the sample was cooled below 4.2 K [1].

Onnes realized that the new phenomenon represented a new physical state and termed it the superconductive state. Thereafter, the phenomenon of vanishing of electrical resistivity of materials below a particular low temperature is called superconductivity and the materials which exhibit this property are called superconductors. The temperature at which the transition from the normal state to the superconducting state occurs is called the critical temperature (T_C). In 1913, he won Nobel Prize in Physics for his research in this field.

After twenty years of the discovery of Onnes, a major breakthrough came in 1933 when Walther Meissner and his student Robert Ochsenfeld discovered an important magnetic property of superconductors. They observed that a magnetic field lower than critical field

(H_C) was suddenly expelled by superconductor specimens on cooling below T_C [1]. In other words, the material becomes fully diamagnetic in the superconducting state.

This is called the Meissner effect and was found to be an intrinsic property of superconductors. It has been widely used for testing the superconducting state. In the superconducting state, an electric current is produced near the surface of sample, in such a way as to create a magnetic field that exactly cancels the external magnetic field.

The superconducting state of a material is decided by three parameters such as temperature, external magnetic field and the current density flowing through the material. These three parameters are coupled together to define the superconducting limits of a material as shown in figure 1.1 which shows that for the occurrence of superconductivity in a material, the temperature must be below the critical temperature (T_C), the external magnetic field must be below the critical field (H_C) and the current density flowing through the material must be below the critical current density (J_C). These define a critical surface as illustrated in figure 1.1, beneath the surface the material is in superconducting state and above the surface the material is in normal state.

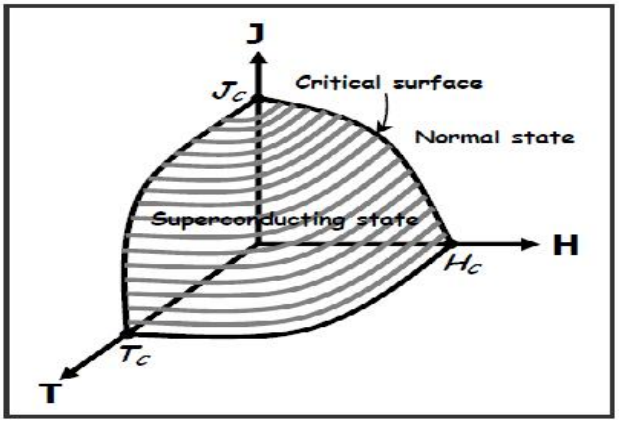

Figure 1.1: Schematic diagram of superconducting domain governed by the critical parameters T_C, J_C *and* H_C

In 1935, Fritz and Heinz London theoretically explained the Meissner effect by postulating two groups of electrons in a superconducting material, the superconducting electrons and the normal state electrons. They employed the Maxwell's equations to develop a set of electrodynamics equations, called the London equations [3,]. According to the London equations, the magnetic field exponentially falls off with increasing distance from the surface of a superconducting sample. This characteristic decay length is called the London

penetration depth (λ) . In 1950, V. Ginzburg and L. Landau developed a theoretical explanation for superconductors based on general symmetry properties [1,2]. Although the Ginzburg-Landau theory explained the macroscopic properties of superconductors, the microscopic properties remained unsolved.

Seven years later, three physicists at the University of Illinois, John Bardeen, Leon Cooper and Robert Schrieffer presented a theoretical explanation for the superconducting state [1]. This theory was widely accepted and is well known as the BCS theory. Based on this theory, despite the Coulomb repulsive forces between the electrons, due to distortion in the crystal structure (phonon mediation), slight attraction between pairs of electrons located near the Fermi surface leads to the production of bonded pairs of electrons, called cooper pairs [1]. Coherence length (ξ) gives approximate spatial dimension of the cooper pair and it sets the length scale on which the superconducting order parameter changes considerably. The BCS theory explained superconductivity in the low temperature and low magnetic field regime. Soon after that, the theory was extended and became useful for high magnetic fields as well [1].

Alexei Alekseevich Abrikosov theoretically investigated the properties of superconductors in external magnetic fields and the way in which magnetic flux can penetrate a superconductor. In 1957 he discovered that superconducting materials can be separated into two groups type-I and type-II superconductors [1]. Type I superconductors show abrupt transition from superconducting Meissner state to normal state above a particular external field which is its critical field (H_C), whereas for type-II superconductors there are two critical fields, the lower critical field (H_{C1}) and the upper critical field ($H_{C\ 2}$). If the external magnetic field is lower than H_{C1}, the field is completely expelled and the material behaves the same as a type-I superconductor. By increasing the field above H_{C1} up to H_{C2}, the flux partially penetrates into the superconductor as vortices. As the field increases above H_{C2} the flux totally penetrates the whole sample, and it returns to the normal state.

In 1962 Brian D. Josephson, a 22 year old British student at Cambridge University, predicted that electric current could flow between two superconducting materials separated by a thin (a few nano meter thick) insulating layer or weak link via a tunneling process [1]. Later, his prediction was experimentally confirmed and became known as the Josephson Effect. A significant breakthrough then was made in 1986 by George Bednorz

and Alex Müller, when they made a ceramic superconductor LaBaCuO with a critical temperature of 30 K [3]. Subsequently, by substitution of yttrium for lanthanum another ceramic superconductor with a critical temperature of 92 K was discovered [4].Since the critical temperature of the material was considerably higher, it facilitated the use of liquid nitrogen, a cheaper refrigerant.

Iron-based superconductors (FeSC) are iron-containing chemical compounds whose superconducting properties were discovered in 2008. FeSe is the simplest iron-based superconductor but with diverse properties [5]. It starts to superconduct at 8 K at normal pressure but its critical temperature (Tc) is dramatically increased to 38 K under pressure and by means of intercalation. The combination of both intercalation and pressure results in re-emerging superconductivity at 48 K. [6, 7]

Tellurium (Te) is a chemical element with symbol Te and atomic number 52. It is a brittle, mildly toxic, rare, silver-white metalloid. Tellurium is chemically related to selenium and sulfur. It is occasionally found in native form as elemental crystals. Te substitution for Se in FeSe enhances *T*c in spite of a negative chemical pressure effect [8, 9]. Density functional calculations of FeSe and FeTe indicated that the strength of spin density wave (SDW) in FeTe and the possibility of a higher *T*c in doped FeTe or Fe (Se,Te) alloy compared to FeSe. According to some experimental works the *T*c increased with Te substitution up to 75 %. The enhancement of *T*c in Te-substituted FeSe may be explained by the results of the density functional calculations. [10]

1.2 Statement of the problem

Superconducting critical temperature is not yet raised to somewhere near the room temperature. Different experimental and theoretical methods have been employed to do so and also to understand the theory of superconductivity. Electronic structure calculation can indicate some properties of the superconducting material. But the theory behind the superconductivity of materials is not well understood. The mechanism in which the superconductivity of material is governed differ even for a materials of the same family.

Hence, the main aim of this research is to understand the effect of Te substitution on electronic property of FeSe superconductor.in this work we attempt to see the effect of 25% and 50% substitution of Te on the Se site. Density functional theory (DFT) will be

employed to calculate the band structure of this compound computationally. The result may explain experimental reports.

1.3 General objective

The general objective of this work is to study the effect of Te substitution on electronic property of iron selenide (FeSe) using the density functional theory (DFT).

Specific objectives

The specific objectives of this work are:

- To obtain the DOS and band structure of tellurium substituted iron selenide ($FeSe_{0.5}Te_{0.5}$, $FeSe_{0.75}Te_{0.25}$)
- To compare the band structure of the undoped FeSe with that of the doped one
- To calculate the superconducting critical temperature.
- To determine the general properties of tellurium substituted iron selenide superconductor in depth

Chapter 2

Review of literature

2.1 Historical background of superconductivity

The phenomenon of superconductivity, in which the electrical resistance of certain materials completely vanishes at low temperatures (this temperature is called transition temperature or critical temperature), is one of the most interesting and sophisticated in condensed matter physics. It was first discovered by the Dutch physicist Heike Kamerlingh Onnes, who was the first to liquefy helium (which boils at 4.2 Kelvin at standard pressure). In 1911 Kamerlingh Onnes and one of his assistants discovered the phenomenon of superconductivity while studying the resistance of metals at low temperatures. They studied mercury because very pure samples could easily be prepared by distillation. The resistivity behavior as a function of temperature is shown in Fig.1.1.

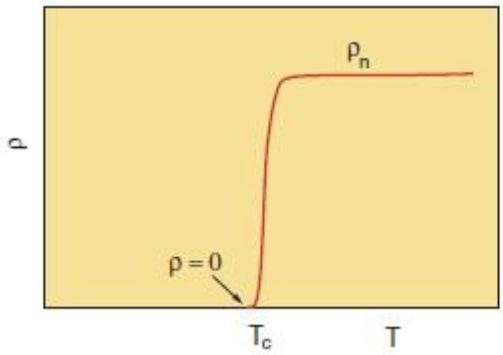

Figure 2.1: Below the transition temperature, the resistivity drops to zero.

Superconductivity is a very curious phenomenon characterized by a phase transition at a critical temperature (Tc) in which the conducting phase is in equilibrium with the superconducting phase. The most important properties of the superconducting phase are: zero resistance, ideal diamagnetism (Meissner effect), magnetic flux quantization and persistent current in superconducting rings, cylinders or coils [11].

According to classical physics, part of the resistance of a metal is due to collisions between free electrons and the crystal lattice's vibrations, known as **phonons**. In addition, part of the resistance is due to scattering of electrons from impurities or defects in the conductor. As a result, the question arose as to why this does not happen in superconductors? For one century superconductivity has been a great challenge to theoretical physics. The first successful set of phenomenological equations for superconducting metals was given by F. London in 1935. Yet, in 1950, almost 40 years after the discovery of this phenomenon, there was not any adequate microscopic theory of superconductivity. However, by 1935, single elements necessary to a successful theory to explain superconductivity was known to theorists. The peculiar condensation of a Bose-Einstein gas was predicted by Einstein in 1925. The idea that pairs of fermions can combine to form bosons has been known since 1931. In 1950 the most relevant ideas of superconductivity have been summarized by F. London in his famous book "Superfluids", volume 1. At last, BCS (bardeen cooper and schriefer) theory was the first successful theory to explain the microscopic mechanisms of superconductivity in metals and alloys. The central feature of the BCS theory is that two electrons in the superconductor are able to form a bound pair called a **Cooper pair** if they somehow experience an attractive interaction between them [12].

Superconductors were observed to exclude magnetic fields, an effect called the Meissner effect, after the person who discovered it. This turned out to be a very important observation since this behavior was different from that of a regular metallic conductor. The Meissner effect indicated that superconductivity could not be merely thought of as better or improved conductivity - a new mechanism had to be proposed. The Meissner effect indicated that magnetism of materials opposed what superconductivity required of materials.

Until 1986, the record transition temperature for a superconductor was 23 K. In that year, Bednorz and Muller synthesized a high temperature superconducting compound La2CuO4 which remains superconducting up to 30 K, and soon afterwards other superconducting cuprate materials were discovered with even higher transition temperatures. High temperature superconductors (HTSCs) are materials that accomplish superconducting state at unusually high temperature.

High-Tc superconductivity at 26 K was found by Kamihara group [15]. in Florine doped LaFeAsO on February 2008. This was the discovery of high-Tc superconductivity in a entirely new class of materials that came to be known as iron-pnictides. This new type of superconductors is based on conducting layers of Iron and a Pnictide (typically Arsenic) and seems to show promise as the next stage of high temperature superconductors. Largely these materials have been called the ferropnictides.

The discovery of superconductivity in FeSe1 has sparked tremendous interest in iron chalcogenides as they are isomorphic to the FeAs-type high *T*c superconductors2-5 but have simpler crystal structure and chemical composition. This should help our understanding of the underlying physics in iron-based superconductors [13].

2.2 The Miessner effect

Meissner and Ochsenfeld (1933) found that if a superconductor is cooled in a magnetic field to below the transition temperature, then at the transition the lines of induction B are pushed out (Fig. 2.2). The Meissner effect shows that a bulk superconductor behaves as if B = 0 inside the specimen.

The demagnetization field contribution is negligible.

$$B = H + 4\pi M = 0 \text{----------} 2.1$$

$$H = -4\pi M$$

Then the magnetic susceptibility is given by

$$\chi = \frac{M}{H} = \frac{-1}{4\pi} \text{----------} 2.2$$

Equation 2.2 shows perfect diamagnetism

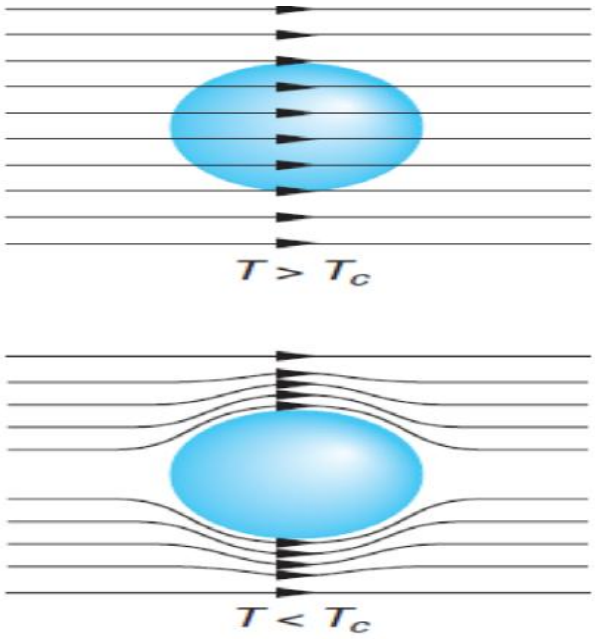

Figure 2.2: The Meissner effect

The result B = 0 cannot be derived from the characterization of a superconductors a medium of zero resistivity. From Ohm's law, E = **ρj,** we see that if the resistivity **ρ** goes to zero while **j** is held finite, then **E** must be zero. By a Maxwell equation $d\mathbf{B}/dt$ is proportional to curl **E**, so that zero resistivity implies $d\mathbf{B}/d\mathbf{t} = 0$, but not B = 0. This argument is not entirely transparent, but the result predicts that the flux through the metal cannot change on cooling through the transition. The Meissner effect suggests that perfect diamagnetism is an essential property of the superconducting state [13].

The BCS theory of superconductivity

The basis of a quantum theory of superconductivity was laid by the classic 1957 papers of Bardeen, Cooper, and Schrieffer. There is a "BCS theory of superconductivity" with a very wide range of applicability, from He3 atoms in their condensed phase, to type I and type II metallic superconductors, and to high-temperature superconductors based on planes of cuprate ions. The BCS theory described some interactions, which include

1. An attractive interaction between electrons can lead to a ground state separated from excited states by an energy gap. The critical field, the thermal properties, and most of the electromagnetic properties are consequences of the energy gap.

2. The electron-lattice-electron interaction leads to an energy gap of the observed magnitude. The indirect interaction proceeds when one electron interacts with the lattice

and deforms it; a second electron sees the deformed lattice and adjusts itself to take advantage of the deformation to lower its energy. Thus the second electron interacts with the first electron via the lattice deformation.

3. The penetration depth and the coherence length emerge as natural consequences of the BCS theory. The London equation is obtained for magnetic fields that vary slowly in space. Thus the central phenomenon in superconductivity, the Meissner effect, is obtained in a natural way.

4. The criterion for the transition temperature of an element or alloy involves the electron density of orbitals $D(E_F)$ of one spin at the Fermi level and the electron-lattice interaction U, which can be estimated from the electrical resistivity because the resistivity at room temperature is a measure of the electron-phonon interaction. For $UD(E_F) \ll 1$ the BCS theory predicts

$$T_C = 1.14\ \theta \exp[-1/\ UD(E_F)] \quad \text{----------2.3}$$

Where θ is the Debye temperature and U is an attractive interaction. The result for T_c, is satisfied at least qualitatively by the experimental data. There is an interesting apparent paradox: the higher the resistivity at room temperature the higher is U, and thus the more likely it is that the metal will be a superconductor when cooled.

5. Magnetic **flux** through a superconducting ring is quantized and the effective unit of charge is $2e$ rather than e. The BCS ground state involves pairs of electrons; thus flux quantization in terms of the pair charge $2e$ is a consequence of the theory.[14]

2.3 Classification of superconductors

High magnetic fields destroy superconductivity and restore the normal conducting state. Depending on the character of this transition, we may distinguish between type I and II superconductors.

The graph shown in Figure 4 illustrates the internal magnetic field strength, Bi, with increasing applied magnetic field. It is found that the internal field is zero (as expected from the Meissner effect) until a critical magnetic field, Bc, is reached where a sudden transition to the normal state occurs. This results in the penetration of the applied field into the interior. Superconductors that undergo this abrupt transition to the normal state above

a critical magnetic field are known as type I superconductors. Most of the pure elements in Figure 2 tend to be type I superconductors.

Type II superconductors, on the other hand, respond differently to an applied magnetic field, as shown in Figure 5. An increasing field from zero results in two critical fields, B_{c1} and B_{c2}. At Bc1 the applied field begins to partially penetrate the interior of the superconductor. However, the superconductivity is maintained at this point. The superconductivity vanishes above the second, much higher, critical field, B_{c2}. For applied fields between B_{c1} and B_{c2}, the applied field is able to partially penetrate the superconductor, so the Meissner effect is incomplete, allowing the superconductor to tolerate very high magnetic fields.

Type II superconductors are the most technologically useful because the second critical field can be quite high, enabling high field electromagnets to be made out of superconducting wire. Most compounds shown in Figure 3 are type-II superconductors. Wires made from say niobium-tin (Nb_3Sn) have a B_{c2} as high as 24.5 Tesla – in practice it is lower. This makes them useful for applications requiring high magnetic fields, such as Magnetic Resonance Imaging (MRI) machines. The advantage of using superconducting electromagnets is that the current only has to be applied once to the wires, which are then formed into a closed loop and allow the current (and field) to persist indefinitely – as long as the superconductor stays below the critical temperature. That is, the external power supply can be switched off. As a comparison, the strongest permanent magnets today may be able to produce a field close to 1 Tesla. However, it is possible to obtain up to 24.5 Tesla from a niobium–tin superconductor. There is a misconception amongst some non-specialists that the term "Type II" refers to the copper oxide based high temperature superconductors discovered in the late 1980s. While these are type II superconductors, so are many superconductors discovered before that time.[11]

Element	T_c (K)	Element	T_c (K)	Element	T_c (K)
Al	1.19	Nb	9.2	Tc	7.8
Be	0.026	Np	0.075	Th	1.37
Cd	0.55	Os	0.65	Ti	0.39
Ga	1.09	Pa	1.3	Tl	2.39
Hf	0.13	Pb	7.2	U	0.2
Hg	4.15	Re	1.7	V	5.3
In	3.40	Rh	0.0003	W	0.012
Ir	0.14	Ru	0.5	Zn	0.9
La	4.8	Sn	3.75	Zr	0.55
Mo	0.92	Ta	4.39		

Compound	T_c (K)	Compound	T_c (K)	Compound	T_c (K)
Nb_3Sn	18.1	MgB_2	39	UPt_3	0.5
Nb_3Ge	23.2	$PbMo_6S_8$	15	UPd_2Al_3	2
Cs_3C_{60}	19	YPd_2B_2C	23	$(TMTSF)_2ClO_4$	1.2
Cs_3C_{60}	40	$HoNi_2B_2C$	7.5	$(ET)_2Cu[Ni(CN)_2]Br$	11.5

High-T_c superconductor	T_c (K)	High-T_c superconductor	T_c (K)
$La_{1.83}Sr_{0.17}CuO_4$	38	$Tl_2Ba_2Ca_2Cu_3O_{10+x}$	125
$YBa_2Cu_3O_{6+x}$	93	$HgBa2Ca_2Cu_30_{8+x}$	135
$Bi_2Sr_2Ca_2Cu_3O_{10+x}$	107	$Hg_{0.8}Tl_{0.2}Ba_2Ca_2Cu_30_{8.33}$	134

Table 2.1:The critical temperatures of some superconductors.

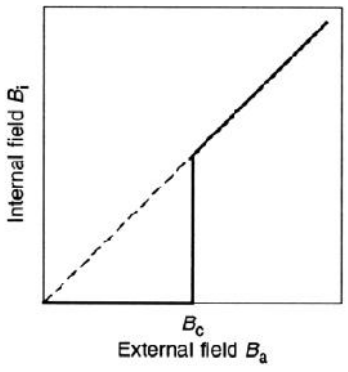

Figure 2.3:Type-I superconductor

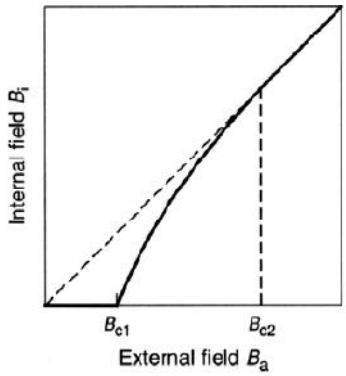

Figure 2.4:Type-II superconductor

2.4 The iron based superconductors

Fe-based superconductors were discovered in 2008. This discovery with values up to 56K, generated a new belief in the field of superconductivity. Till its discovery, high temperature superconductivity in cuprates, created a prejudice that Cu-oxides are essential building

blocks for a high temperature superconducting material. These Fe based superconductors do not contain Cu-O planes (some of the materials are even O free). Iron pnictide and chalcogenide (FePn/Ch) superconductors have Fe electrons at the Fermi surface together with an unusual Fermiology that can change rapidly with doping. This may lead to very different normal and superconducting state properties compared to those in standard electron-phonon coupled ‘‘conventional’’ superconductors. There are a large number of evidences showing that superconductivity, magnetism, orbital fluctuations are intimately related and coexist in these materials although the mechanism of superconductivity in these compounds is still unknown. The electronic specific heat,$2\Delta/k_BT_C$ ratio, phase diagrams, isotope effect, crystal structures and there correlation to T_C from various available experimental data.

As iron has strong local magnetic moment, it is usually considered deleterious to superconductivity, the recent discovery of high temperature superconductivity at 26 K in LaFeAsO doped with F on the oxygen site in 2008 is one of the exceptions [15]. Other such examples of exceptions are Th_7Fe_3 (T_C =1.8 K)[16], U_6Fe(T_C =3.9 K)[17], $Lu_2Fe_3Si_5$(T_C=6.1K)[18]. Furthermore, Fe itself under pressure is a superconductor with T_C =1.8 K at 20 Gpa[19]. Fe based superconductors do not have any copper-oxide layers which are thought to be essential ingredient for high T_C cuprates. In fact some of the Fe-based superconductors with record of around 56 K, neither contains Cu nor O, e.g., $Gd_{0.8}Th_{0.2}FeAsO$, $Sr_{0.5}Sm_{0.5}FeAsF$ and $Ca_{0.4}Nd_{0.6}FeAsF$ [20]. Fe based superconductors also known as Fe-pnictides (‘‘FePn ’’ where Pn is As or P) have extended its family to include iron chalcogenides (‘‘FeCh’’ where Ch includes S,Se and Te). We shall firstly discuss about structural aspects and its correlation to T_C in these compounds below. Strikingly, many papers have been published about Fe-based superconductors. These suggest that the superconductivity may be related to the coexistent magnetism, orbital fluctuation and primarily not due to phonon.

The properties of the FePn/Ch superconductors are fundamentally different both from those of a conventional electron-phonon coupled superconductor and from those of the high T_C cuprates. It is accepted (by now) that the superconducting pairing symmetry in high T_C cuprates is $d_{x^2-y^2}$ kind corresponding to l=2 orbital angular momentum. Such type of unconventional order parameter allows finite electronic excitations remaining even at

$T \rightarrow 0$. This is in contrast to a clean conventional superconductor, where the electronic excitations are suppressed (exponentially) below T_C by opening a gap in the electronic spectrum. Such existence of finite electronic excitations well below T_C is also found from numerous experimental studies in Fe-based superconductors. While superconducting order parameter symmetry and the mechanism responsible are still unknown, it is apparently not conventional wave symmetry. Neutron scattering measurements provide convincing evidence for a sign change in the superconducting energy gap on different parts of the Fermi surface in a number of compounds. Thus Fe-based superconductors are not only unconventional but also different from high- T_C cuprates. We shall argue that Fe-based superconductors are *different* from others in a number of ways; (a) coupling of magnetism, superconductivity and orbital degrees of freedom --- possible connection of structural transition to orbital degree than lattice. In a number of cases structural and magnetic transition temperatures are identical. (b) The specific heat jump scales very differently than other conventional as well as unconventional superconductors. (c) They have very different Fermi-ology made of Fe-d electrons than other classes of superconductors which changes drastically with electron or hole doping. (d) Although numerous theoretical/experimental data suggest to multiband Fermi surface and multi-gap, there are strong spectroscopic evidences of two –gaps (i) one large and (ii) small gaps giving rise to two sets of $2\Delta/k_BT_C$ ratios, averaging about 7 and 3 respectively. (d) Unlike conventional superconductors Fe-based superconductors do not exhibit any O isotope effect but Fe isotope effect instead. (e) The spin susceptibility in a large number of compounds produces linear temperature dependencies. (f) Spin resonance energy which is also observed in high T_C cuprates, scales with T_C linearly. As of recent articles iron based superconductors are classified in tho the following groups.

1111 family

LaFeAsO and the 1111 family of Iron-pnictides crystallizes in the ZrCuSiAs type structure, (space group P4/nmm). In this structure, two-dimensional layers of edge- sharing $FeAs_{4/4}$ tetrahedral alternate with sheets of edge-sharing $LaO_{4/4}$ tetrahedral as shown in Fig 2.6(a) [38]. Because of the differences between the ionic nature of the Ln-O (Lanthanum oxide)bonds and the more covalent Fe-As (iron arsenide) bonds, a distinctive two-

dimensional structure forms, where ionic layers of lanthanum oxide $(LaO)^{+}$ alternate with metallic layers of iron arsenide $(FeAs)^{-}$.

122 family

The ternary iron arsenide BaFe2As2, with the tetragonal ThCr2Si2-type structure space group (space group I4/nmm) contains practically identical layers of edge- sharing FeAs4/4 tetrahedral, but they are separated by barium atoms instead of LaO sheets. This structure is shown in Fig 2.6(b) [36].

111 family

LiFeAs crystallizes into a Cu2Sb-type tetragonal structure containing [FeAs] layer with an average iron valence Fe^{2+} like those for 1111 or 122 parent compounds. This structure is shown in Fig 2.6 (c) [37].

11 family

The PbO-type αFeSe crystal structure is shown in Fig 2.6(d) [5].

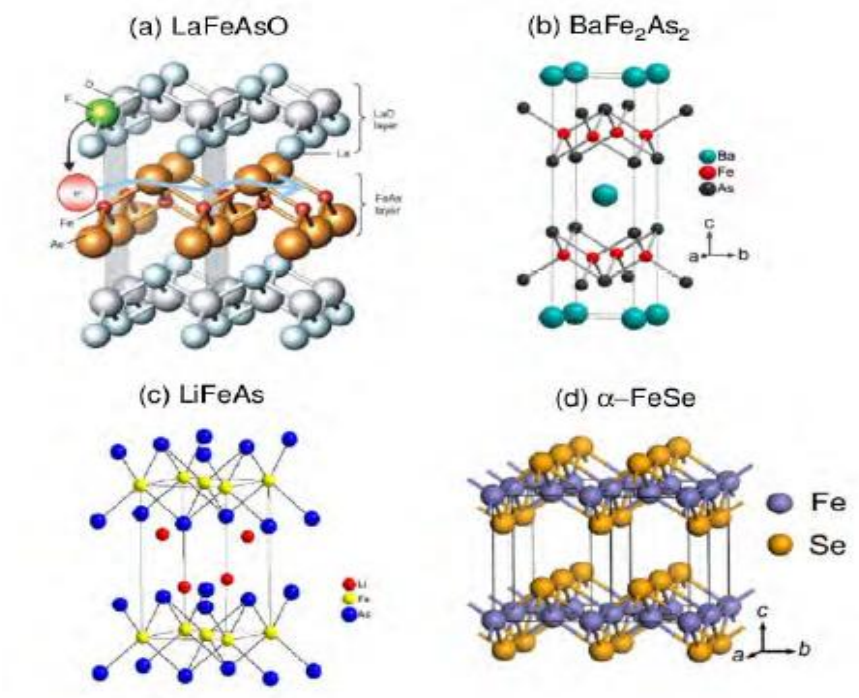

Figure 2.5: Schematic Crystal structure of: (a) LaFeAsO , (b)BaFe2As2 (c) LiFeAs (d) αFeSe.

2.5 Superconducting state of FeSe

FeSe is structurally the simplest of the iron-based superconductors, but is host to some of the richest physics. Shortly after high-Tc superconductivity was found in iron-pnictide

systems by Kamihara et. al.,[15] superconductivity in the Fe-chalcogenide compound FeSe below 8 K was discovered by Hsu et. Al[5]. All these materials share a common structural motif of a square lattice of Fe, bonded to pnictogen or chalcogen ions which sit alternately above and below the plane. The appearance of unconventional superconductivity in the Fe-based systems is commonly thought to arise from a spin fluctuation pairing mechanism, linked with the suppression of spin-density wave ordering observed in the parent compounds. However the unique properties of non-magnetic FeSe provides a challenging test-case for this view, and has generated intense detailed experimental and theoretical investigation of its electronic and magnetic properties.

The superconductivity of FeSe is remarkably tunable. Under applied pressure, Tc reaches 36.7 K at 8.9 GPa [21]. Furthermore, the FeSe layers are held by weak van der Waals bonds that make them susceptible to mechanical exfoliation and chemical intercalation. Ionic gating using field effect layer transistor in thin flakes of FeSe induces dramatic changes in the carrier density and enhances superconductivity towards 43 K [22]. Intercalation has the effect of separating the layers and also effectively dopes them with electrons, and a similarly enhanced Tc can be achieved [23,24].

The recent renaissance in research on FeSe has been mainly driven by significant advances in materials development. Firstly, the discovery of high temperature superconductivity in a monolayer FeSe grown by molecular beam epitaxy on SrTiO3 [25,26] provided an exciting new route towards strongly enhanced superconductivity over 65 K in an two-dimensional iron-based superconductor.

Secondly, it was found that the chemical vapor transport method[27,28,29] could yield mm-sized plate-like single crystals free of impurity phases and close to stoichiometry, enabling detailed study of the intrinsic physics of bulk FeSe.

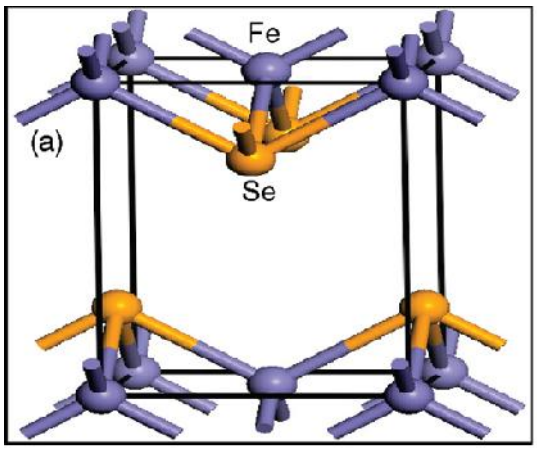

Figure 2.3 Crystal structure of FeSe

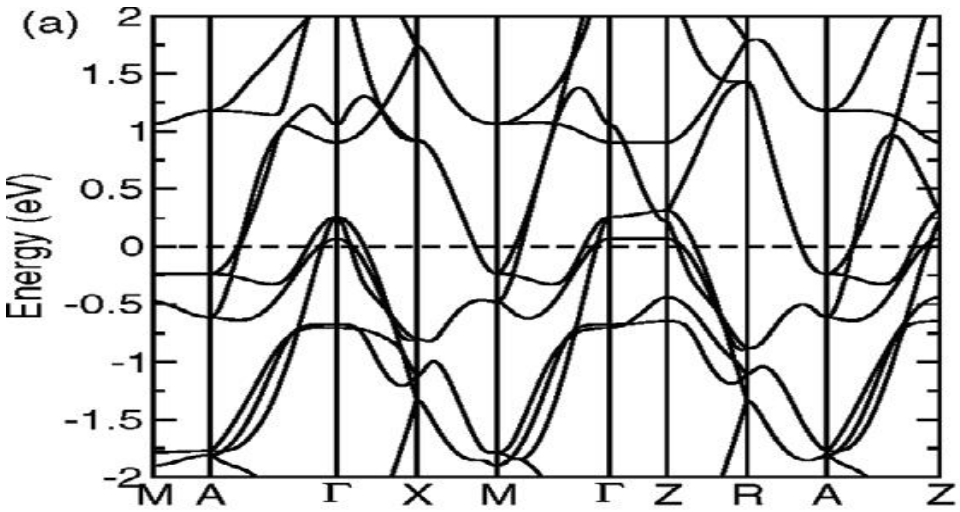

Figure 2.4: Band structure of FeSe

2.6 Density functional theory (DFT)

The first principles approach to condensed matter theory is widely used. It starts from the very basic principles that materials are made of atoms. These atoms are again made of a positively charged nucleus and a number of negatively charged electrons. The interactions between atoms are determined by the interactions of the constituent electrons and nuclei that form the basic interaction. Thus if we can model interactions accurately, then most of the complex physical properties can be understood. Thus the *ab initio* calculation or first-principles calculation do not depend upon any external parameters except the atomic numbers of the constituent atoms to be modelled and cannot therefore be biased by preconceptions about the final result. Such calculations are reliable and can be used with confidence to predict the behaviour of nature.

Density functional theory (DFT) is the basic theory of electronic structure calculations in Condensed Matter Physics. It was so challenge to approximate functional and computational cost. In 1990's there are widely used functional that give a quite reasonable accuracy with the affordable computational cost. In simple language, Density functional theory is a completely different in terms of its approaching any interacting problem that by mapping it exactly to a non-interacting problem that gives an alternative way to tackle the problem. Thus DFT is a ground-state theory in which the charge density is the relevant physical quantity. DFT is very successful in describing structural and electronic properties in materials science and chemical science.

Density functional theory is developed based on the Hohenberg-Kohn theorem. There are two parts in Hohenberg-Kohn Theorem[30].

2.6.1 Hohenberg-Kohn Theorem –I:

This theorem states that the external potential *Vext*(r) is determined (within a trivial additive constant) by the electron density ρ(r).

It implies that for a given density there will be a single *Vext*(r). In other words, there cannot be two *Vext*(r) for a given ρ(r). Thus, this theorem demonstrates that the electron density specifies uniquely the Hamiltonian operator.

In consequence, an alternative statement of the first Hohenberg Kohn theorem is that any ground state expectation value corresponding to an observable, $\hat{O}$is a functional of the density, [30]

$$O[\rho] = \left\langle \psi[\rho] \middle| \hat{O} \middle| \psi[\rho] \right\rangle$$

2.6.2 Hohenberg-Kohn Theorem –II:

The second Hohenberg Kohn theorem states that the functional $F_{HK}[\rho]$ that delivers the ground state energy if and only if the input density is the true ground state density[30].

In other words,

For a trial density ρ'(r) such that ρ'(r)$\geq$ 0 and $\int \rho'(r)\,dr = N$

$$E[\rho] \leq E[\rho']$$

Where E[ρ'] is the energy functional

$$E[\rho'] = \int \rho'(r) V_{ext}(r) dr + F_{HK}[\rho']$$

2.6.3 Kohn-Sham equations

We know that a solid consists of heavy positively charged particles (nuclei) and lighter negatively charged particles (electrons). The nuclei are much heavier and therefore much slower than the electrons. We can consider the nuclei are at fixed positions. So, the nuclei become the external potential to the electrons. This is the Born-Oppenheimer approximation. In the further discussion, we use the atomic units (that is e = me = ħ = 1; $4\pi\epsilon_o$=1). Now, after Born-Oppenheimer approximation, we can see the Solid is generally a system of interacting electrons in the field of fixed ions described by the Hamiltonian, [30]

$$\hat{H} = \sum_{i=1}^{N}\left(-\frac{1}{2}\nabla_i^2\right) + \sum_{i=1}^{N} V_{ext}(r_i) + \sum_{i<j}^{N}\frac{1}{r_{ij}} \quad \text{----------2.4}$$

Where "*rij*" is the separation between i^{th} and j^{th} electrons;

$V_{ext}(r_i) = -\sum_{I=1}^{M}\frac{Z_I}{r_{iI}}$ is the external potential acting on i^{th} electron due to the M nuclei and "r_{iI}" is the separation of i^{th} electron and I^{th} nucleus.

A stationary electronic state is then described by a wave function Ψ (r_1, r_2,.....r_i.....r_N) satisfying the many electron Schrödinger equation,

That is

$$\hat{H}\psi = E\psi$$

$$[\hat{T} + \hat{V}_{ext} + \hat{V}_{ee}]\psi = E\psi \quad \text{----------2.5}$$

Hohenberg and Kohn proved that the total energy of a system in the presence of the static external potential is unique functional of the charge density.

$$E[\rho] = T[\rho] + V_{ee}[\rho] + V_{ext}[\rho]$$

$$E[\rho] = F_{HK}[\rho] + \int \rho(r) V_{ext}(r) d^3r$$

Here the term,

$$T[\rho] + V_{ee}[\rho] = F_{HK}[\rho]$$

is same for all solid and thus it is universal. This does not depend on the particular system under consideration and is called Hohenberg-Kohn functional.

In the non-interacting case, *Vee* = 0,

Thus the ground state energy $E[\rho]$ has a kinetic contribution and a contribution from the external potential.

$$E[\rho] = T_o[\rho] + V_{ext}[\rho] = T_o[\rho] + \int \rho(r) V_{ext}(r) d^3r$$

Again, the ground state wave function of the non-interacting system can be written as a Slater determinant with the orbitals satisfying the single particle Schrodinger equation,

$$\left[-\frac{1}{2}\nabla^2 + V_{ext}(r) \right] \phi_m^o(r) = \varepsilon_m^o \phi_m^o$$

The ground state density is then given by a sum over occupied states,

$$\rho(r) = \sum_m^{occup} \left| \phi_m^o(r) \right|^2$$

Where the orbital ϕ_m^0 are normalized so that the density satisfies the correct condition to the number of particles N.

Thus, we can write the ground state energy for this non-interacting case as

$$\sum_m^{occup} \varepsilon_m^o - T_o[\rho] + \int \rho(r) V_{ext}(r) d^3r$$

Now, for the interacting case, we can represent the energy functional $E[\rho]$ for a many electron system in the form,

$$E[\rho] \quad T_O[\rho] + \int \rho(r) V_{ext}(r) d^3r + \frac{1}{2} \iint \frac{\rho(r_1)\rho(r_2)}{|r_1 - r_2|} d^3r_1 d^3r_2 + E_{XC}[\rho(r)]$$

Where

$\frac{1}{2} \iint \frac{\rho(r_1)\rho(r_2)}{|r_1 - r_2|} d^3r_1 d^3r_2 - V_H[\rho]$ is the Hatree energy.

and $E_{XC}[\rho(r)]$ is the exchange correlation energy that contains all the contributions not taken into account in the kinetic energy functional of non-interacting electron gas, the external and the Hatree energy respectively.

Thus, we can write the analogous equation [equation (5) for non-interacting case] for the interacting electron system as

$$\left[-\frac{1}{2}\nabla^2 + V_{eff}(r) \right] \phi_m(r) = \varepsilon_m \phi_m$$

Where the single particle wave functions $_m(r)$ are the N lowest energy solutions of the above equation (9) called the Kohn Sham equations and $_m(r)$ are the Kohn Sham orbital that reproduce $\rho(r)$ of the original many-body problem.

$$V_{eff} - V_{ext}(r) + \int \frac{\rho(r')}{|r \quad r'|} d^3r' + \frac{\delta E_{XC}[\rho]}{\delta\rho(r)}$$

That is

$$V_{eff} = V_{ext}(r) + V_H(r) + V_{XC}(r)$$

Where

$V_H(r) = \int \frac{\rho(r')}{|r - r'|} d^3r'$ is the Hatree potential.

$V_{XC}(r) \quad \frac{\delta E_{XC}[\rho]}{\delta\rho(r)}$ is the exchange correlation potential.

2.6.4 Easy Steps for Computational DFT

We recall the representation of total energy of the interacting electrons system,

$$E[\rho] = T_o[\rho] + \int \rho(r) V_{ext}(r) d^3r + \frac{1}{2} \iint \frac{\rho(r_1)\rho(r_2)}{|r_1 \quad r_2|} d^3r_1 d^3r_2 + E_{XC}[\rho(r)]$$

So, we have from above equation,

$$V_{eff} = V_{ext}(r) + V_H(r) + V_{XC}(r)$$
$$V_{ext} = V_{eff}(r) - V_{XC}(r) - V_H(r)$$

Incorporating this expression in the above equation, we can write as

$$E[\rho] = \sum_m^{occup} \varepsilon_m^o - \frac{1}{2} \iint \frac{\rho(r_1)\rho(r_2)}{|r_1 - r_2|} d^3r_1 d^3r_2 - \int V_{XC}(r)\rho(r) d^3r + E_{XC}[\rho(r)]$$

The above equation gives the final expression for the ground state energy of the system of interacting electrons. This is the expression used in computational calculation to determine the ground state energy functional for the interacting system of electron. [30]

2.6.5 Local-density approximation (LDA)

he exchange correlation energy is not helpful for practical calculations and one needs to use an approximation for this quantity. While DFT itself does not give any hint on how to construct approximate exchange-correlation functionals, it holds both the promise and the challenge that the true Exc is a universal functional of the density, i.e., it has the same functional form for all systems. On one hand this is a promise because an approximate functional, once constructed, may be applied to any system of interest.

On the other hand this is a challenge because a good approximation should perform equally well for very different physical situations.

Both the promise and the challenge are reflected by the fact that the simplest of all functionals, the so-called local density approximation (LDA) has remained the

approximation of choice for quite many years after the formulation of the Kohn-Sham theorem. In LDA, the exchange correlation energy is given by

$$E_{xc}^{LDA}[n] = \int d^3r\, n(\boldsymbol{r}) e_{xc}^{\mathrm{unif}}(n(\boldsymbol{r}))$$

where e_{xc}^{unif}(n) is the exchange-correlation energy per particle of an electron gas with spatially uniform density n. It can be obtained from quantum Monte Carlo calculations and simple parameterizations are available. By its very construction, the LDA is expected to be a good approximation for spatially slowly varying densities. Although this condition is hardly ever met for real electronic systems, LDA has proved to be remarkably accurate for a wide variety of systems [41].

2.7 Applications

With the discovery of High Temperature Superconductors (HTS) the commercial applications involving these materials became very interesting. In fact, the high power density and electrical efficiency of superconductor wire results in highly compact, powerful devices and systems that are more reliable, efficient, and environmentally benign. Thus, their application involves areas such as, medicine, transportation electrical grids and industry

One of the main applications of the superconductivity is in transportation, more specifically in trains through the magnetic levitation. Due to this, the friction between the train and the rail is eliminated. As a result, these trains can achieve high speed with lower consumption and noise. The maglev train in Shanghai that began commercial operations in 2004 is one example of a real application where this technology is used.

The use of superconductivity for the electricity transport is another area where this technology can be used with several benefits. One of the main advantages is the lack of resistive losses improving in this way the efficiency of the energy transportation. However, there are other advantages such as, higher transport capability, smaller overall size leading to lower impact on soil, possibility of using exiting corridors and lower impact on nature. Due to this, in the last years it started the use of semiconductors in electricity transport.

Besides the use of superconductivity for the electricity transport, it is also possible to use this technology in other electrical power systems. Examples of this are the use of superconductivity in transformers, generators and motors. The interest to use the

superconductivity in transformers started in 1960s with the appearance of low-temperature superconductors and their use in the transformer windings. In fact, several manufacturers around the world, among them the European (ABB and Alstom), the Japonese (KEPC) and Americans (Westinghouse) (USA) made some tests with these equipment's. However, with the discovery of HTS materials in 1986, this interest increased since allowed to eliminate the cumbersome cooling devices. Several advantages are associated with HTS transformers, namely, greater efficiency, ability to run above rated power without affecting transformer life, smaller, lighter and quieter[41].

2.8 Quantum ESPRESSO

Quantum ESPRESSO: Quantum opEn-Source Package for Research in Electronic Structure, Simulation, and Optimization, is an integrated software suite for first-principle simulations, using density-functional theory (DFT), a plane waves (PW) basis set and pseudopotentials (PP).

The main goals of quantum ESPRESSO are

- Innovation in methods and algorithms
- Efficiency on modern computer architectures
- A great effort is also devoted to user friendliness and to the formation of a users' and developers' community

Advantages:

- Everybody – including commercial entities – can contribute.
- Nobody can "steal" the code and give nothing back to the community.

Quantum ESPRESSO is a *distribution* of packages, rather than a single monolithic tightly integrated package. The core distribution contains the two main packages:

- PWscf: self-consistent electronic structure, structural optimization, molecular dynamics on the electronic ground state
- CP: variable-cell Car-Parrinello molecular dynamics.

They share a common installation method, input format, PP format, data output format, large parts of the basic code.

What can quantum ESPRESSO do?

• Structural modeling (equilibrium structures of molecules, crystals,surfaces)

• Dynamical modeling (first-principles molecular dynamics) either on the electronic ground state (Born-Oppenheimer) or with fictitious electronic kinetic energy (Car-Parrinello)

• Chemical reactivity and transition-path sampling, using Nudged Elastic Band (NEB) method

• Linear response functions (vibrational and dielectric properties), plus some non-linear ones (third-order force constants and dielectric response, non-resonant Raman)

• Computational microscopy (STM)

Chapter 3

Computational methods

In this work the calculations are performed employing the known mathematical tool that is the density functional theory (DFT) through the QUANTUM ESPRESSO (QE) program. We adopt non relativistic pseudopotentials to model the electron-ion interactions and the local-density approximation (LDA) of the exchange-correlation potential [32]. We selected the suitable pseudopotentials from QE homepage for Fe, Se and Te from many alternatives in the library that enables us to obtain a high quality result. For Fe we used ***Fe-pbesol-spn-rrkjus-psl.0.2.1.UPF,*** for Se we used ***Se-pbesol-n-rrkjus-psl.0.2.UPF*** and for Te ***Te-pbesol-dn-rrkjus-psl.0.2.2.UPF*** pseudopotentials in order to make our calculations. The energy convergence is checked with respect to the cutoff energies and k-point sampling. The cutoffs for wave functions and charge density are 64.0Ry and 782Ry, respectively, within the framework of the density functional theory (DFT) [33] in their linear response method [34].

To obtain the structures for different concentration of Se and Te, we used lattice parameters of a=b=3.765[a.u], c=5.51[a.u] [39]. There are two Fe atoms, one Se atom and one Te atom for the $FeSe_{0.5}Te_{0.5}$. On the other hand, there are four Fe atoms, three Se atom and one Te atom for the $FeSe_{0.75}Te_{0.25}$. We optimized the structural parameters for different concentrations of Se and Te. Then after we calculate the electronic and lattice dynamical properties of FeSe based on the optimized structure.

The bands are plotted along the high symmetry direction in the conventional tetragonal-TET Brillouin zone, the lattice following the path $\Gamma - X - M - \Gamma - Z - R - A - Z$ [40] as shown in fig 3.1. 121 k-points mesh in the Brillouin zone was used. The DOS calculation were performed using tetrahedron method.

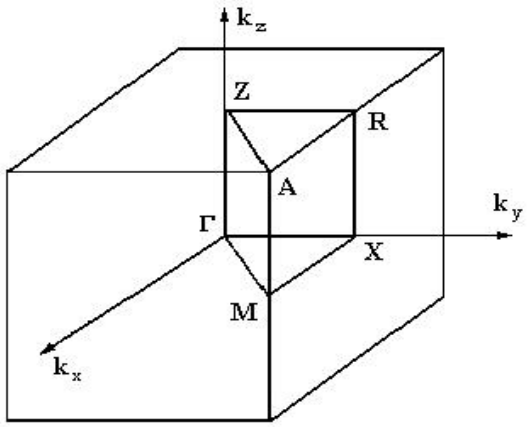

Figure 3.1Brillouin zone of TFT with path: Γ – X – M – Γ – Z – R – A – Z

In this research, we focused more on the effect of tellurium doping to calculate transition temperature. We describe our computational methods and give structural parameters given by some articles for FeSe compositions in the tetragonal phase of the PbO-type (P4/nmm). The results of band structure calculations corresponding to different concentrations of Te and Se. we used ms-word to write the thesis, grace software to plot the band structure. DOS and different graphs of FeSe compound and XCrySDen software is used to draw the crystal structure of FeSe.

Chapter 4

Result and Discussion

In this research we study the effect of Te substitution on Se site. We particularly simulated the band structure and density of electron state (DOS). We have studied $FeSe_{1-x}Te_x$ superconductors with x = 0.25 and 0.5. Based on the initial file we prepared and using XCrySDen software we obtained the crystal structure as shown in the figure. Fig 4.1 and Fig 4.2. The structure is the right structure we expected. The band structure of FeSe is calculated in the space group P4/nmm with non-spin polarized orbitals. The unit cell of FeSe in the space group P4/nmm consists of two Fe atoms and two Se atoms. Similarly, there are of two Fe atoms and two Se atoms in FeTe, two Fe atoms, one Se atom and one Te atom for the $FeSe_{0.5}Te_{0.5}$. On the other hand, there are four Fe atoms, three Se atom and one one Te atom for the $FeSe_{0.75}Te_{0.25}$.

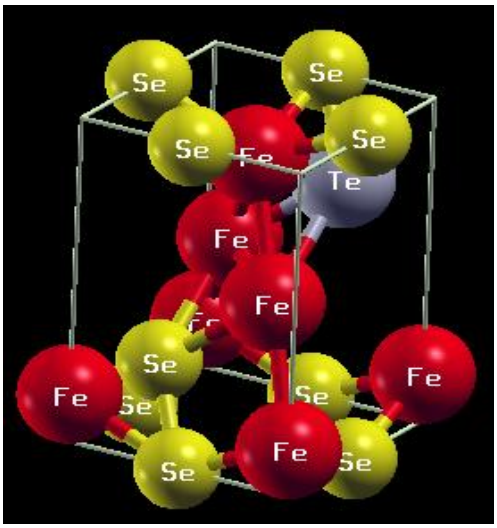

Figure 4.1: Crystal structure of $FeSe_{0.75}Te_{0.25}$

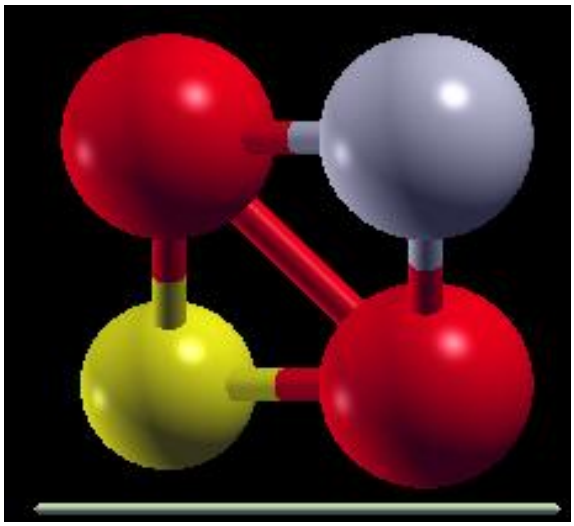

Figure 4.2: Crystal structure of $FeSe_{0.5}Te_{0.5}$

The band structure we found for FeSe and FeTe (fig 4.3 and 4.4) that is at x=0 and x=1 is similar to the already reported one. This is a good step to do for x=0.5 and x=0.25. From fig

4.5 and 4.6 one can see that the band structure has similar nature with that of most iron based superconductors. As we see from the band structure (in fig 4.3-4.6) the electronic structure of all species near the fermi energy contains mainly the Fe-3d states as can be seen from the distinct orbital character of bands which is very common in iron-based superconductors. However, the bands at the Fermi level (E_F) have also contributions from the pz orbitals, which indicates that Te/Se-p orbitals may play a substantial role in superconductivity as well.

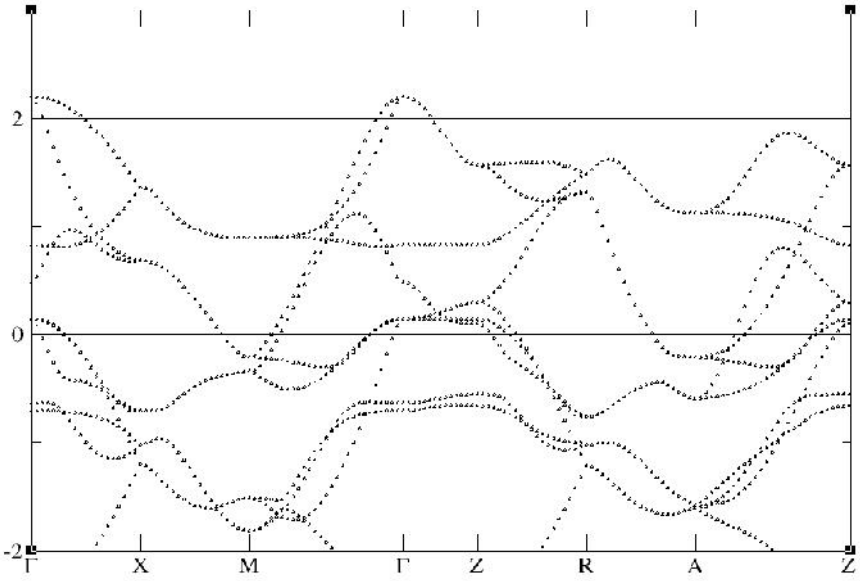

Figure 4.3: Band structure of FeSe

Tellurium (Te=0.5) substituted band structure(fig 4.6) shows unique properties. The electron band at M is at higher energy compared to the Γ point. When we compare the height of hole bands at Γ point the $FeSe_{0.5}Te_{0.5}$ is a bit higher than that of the FeSe (fig 4.3 and fig 4.6).

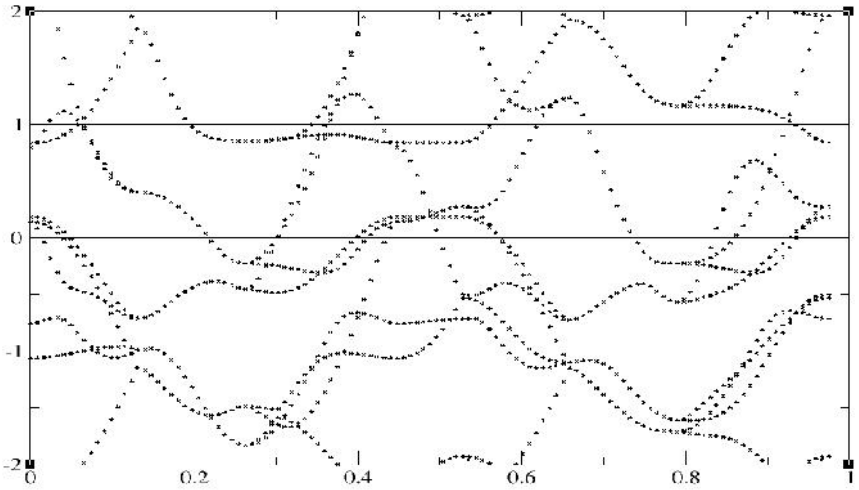

Figure 4.4: band structure of FeTe

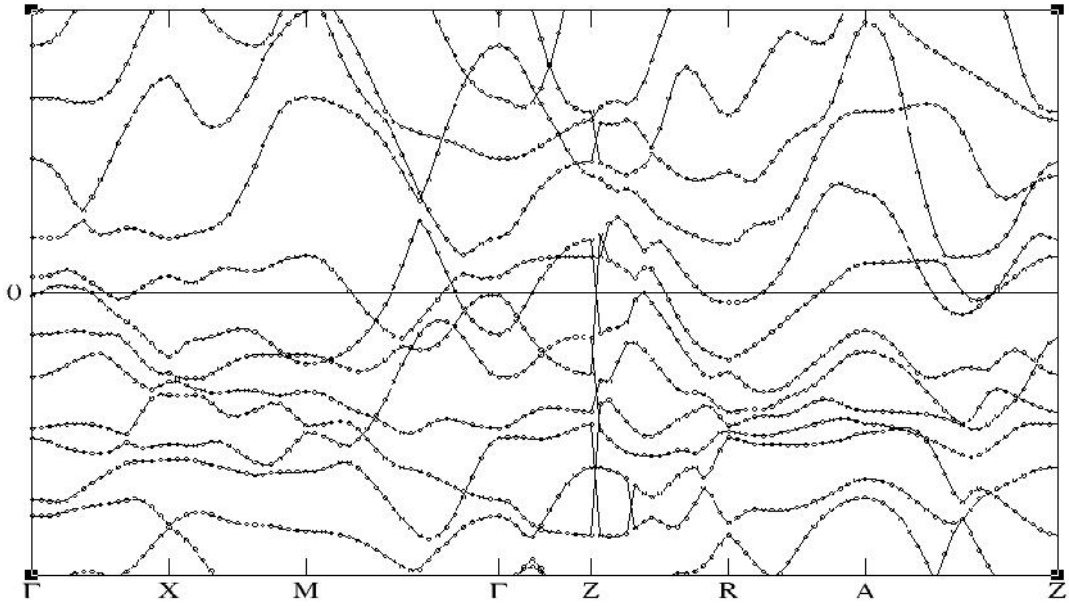

Figure 4.5: band structure of $FeSe_{0.75}Te_{0.25}$

In FeSe and $FeSe_{0.5}Te_{0.5}$, it is observed that many hole bands are crossing the fermi level indicating that the superconductivity of the materials is due to hole doping (fig 4.3 and fig 4.6). On the other hand in $FeSe_{0.75}Te_{0.25}$ only few bands are crossing the fermi level indicating that the compound may have a semi metallic property. And also the sharp bands shows that the compound is not in the superconducting state (fig 4.5). we also observed

many bands in $FeSe_{0.75}Te_{0.25}$ as compared FeSe due to the increment in the unit cell due to the introduction of Te.

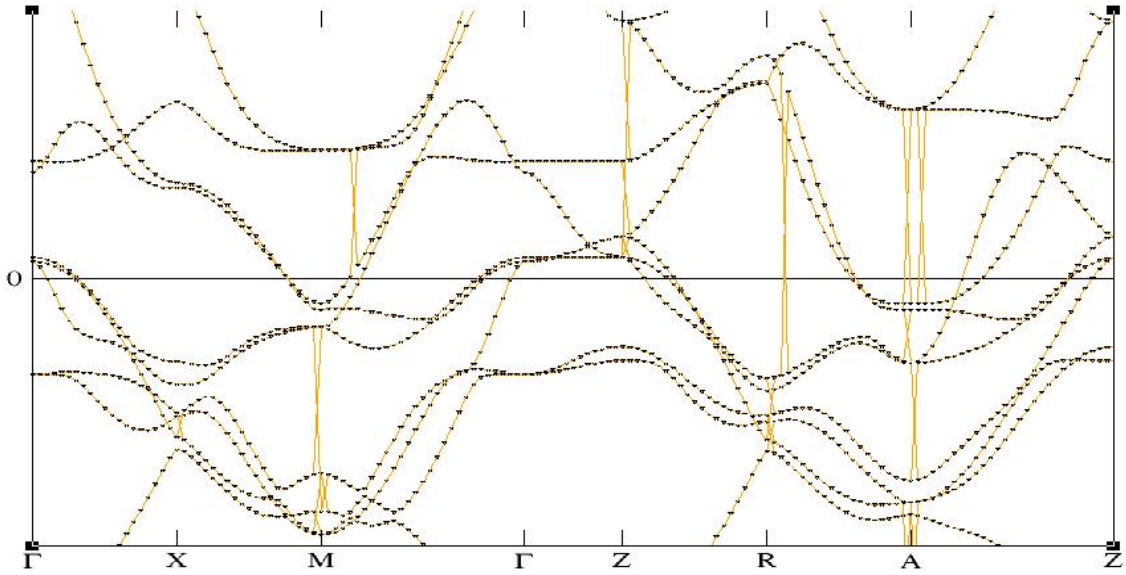

Figure 4.6 Band structure of $FeSe_{0.5}Te_{0.5}$

In $FeSe_{0.5}Te_{0.5}$ from Γ-Z there is a flat band which is not seen at $FeSe_{0.75}Te_{0.25}$, this property may explain the nature of superconductivity on $FeSe_{0.5}Te_{0.5}$.

The value of DOS at the fermi level for FeSe is N (E_F)$\approx 2.69\, states/(eV.cell)$. Then the T_C was calculated using the Debye temperature (Θ_D =210K) and the McMillan equation and it was found to be 8K. Then applying DFT as implemented in QE, we simulated the DOS of the substitution of Se by Te (x=0.5) as shown in Fig 4.7. The reading of the calculated value of DOS at the fermi level amounts to N (E_F)$\approx 3.84\, states/(eV.cell)$ suggesting a small increase of electronic density with raising tellurium content.

Using the reported value of the Debye temperature (Θ_D =246K) and the electron phonon parameter $\lambda \cong 0.92$ the critical temperature is found to be 12.08K according to McMillan equation.

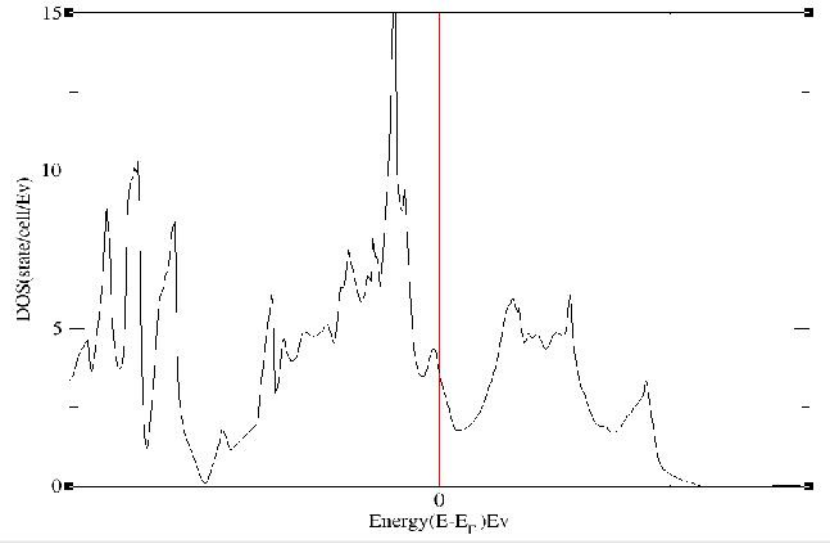

Figure 4.7: DOS of $FeSe_{0.5}Te_{0.5}$

Chapter 5

Conclusions

In this work we present a DFT calculation as implemented in QE. We did the calculation for FeSe and FeTe to compare with the already reported result. We make calculations and simulations to obtain a band structure and DOS with QE code. We have studied the effect of substitution of tellurium on the superconductivity of FeSe within different concentrations. We investigated the changes made in crystal structure, band structure and DOS due to the introduction of Te in the structure of FeSe.

The general properties of the band structure are similar with most of the Iron-Based superconductors that shows multi band nature. The bands are highly affected in the presence of Te. At x=0.5, there is a flat band from Γ to Z direction. At Γ point the hole bands increasing in the energy. It was reported that in $FeSe_{0.5}Te_{0.5}$ due to the reduced Fermi surface nesting, a possible SDW state becomes more unstable than in FeSe. This may be an indication for the enhancement of high T_C in agreement with our result. This can lead to higher values of Tc. From our calculation we noticed that the increment of DOS at fermi level with $FeSe_{0.5}Te_{0.5}$. The density of states at the fermi energy for FeSe is $2.69\ states/(eV.cell)$ whereas the DOS at the fermi energy for $FeSe_{0.5}Te_{0.5}$ $3.84\ states/(eV.cell)$ which enhances superconductivity. The orbital character of bands and projected DOS confirm that the electronic structure near the Fermi energy consists of Fe-3d electrons being slightly hybridized with chalcogenide 3p/4p states.

In general, we can conclude that there is a significant change in critical temperature due to the substitution of Se by Te with value of T_C 12.08K.

References

[1] M. Tinkaham, introduction to superconductivity, 2nd edition, Dover publications, New York (1996)

[2] V. L. Ginzburg, ***Rev. Mod. Phys***. 76, 981 (2004)

[3] G. Bednorz and K. A. Muller, ***Z. Phys. B*** 64, 189 (1986)

[4] M. K. Wu, J. R. Ashburn, C. J. Torng, P. H. Hor, R. L. Meng, L. Gao, Z. J. Huang, Y. Q. Wang and C. W. Chu, ***Phys. Rev. Lett.*** 58, 908 (1987)

[5] F.-C. Hsu; et al., Proc. Natl. Acad. Sci. **105** (38) (2008).

[6] Medvedev, S.; *et al.,*. Nature Materials. 8 (8). (2009).

[7] R. Peng; et al. Physical Review Letters. **112** (10) (2013).

[8] M. H. Fang, *et al*., Phys. Rev. **B 78** -224503 (2008).

[9] K. W. Yeh *et al*., Europhys. Lett. **84**-37002 (2008).

[10] A. Subedi *et al*., Phys. Rev. **B 78** -134514 (2008).

[11] Adir Moysés Luiz, Superconductivity. SCIYO, India (2010)

[12] Adir Moysés Luiz, Superconductivity – Theory and Applications. Intech, Zagreb (2011)

[13] Ravhi S. Kumar *et al.,* J. Phys. Chem*. B* **2010,** *114,* 12597–12606 (2010)

[14] Charles K. Introduction to Solid State Physics 8th ed. John Wiley and Sons.inc New York (2005)

[15] Y. Kamihara, T. Watanabe, M. Hirano and H. Hosono, J. Am. Chem. Soc. **130**, 3296 (2008).

[16] B. T. Matthias, V. B. Compton, and E. Corenzwit, J. Phys. Chem. Solids **19**, 130 (1961).

[17] B. S. Chandrasekhar, and J. K. Hulm, J. Phys. Chem. Solids **7,** 259 (1958).

[18] H. F. Braun, Phys. Lett. **A75**, 386 (1980).

[19] K. Shimizu. *et al*., Nature (London) **412**, 316 (2001).

[20] C. Wang, *et al.*, Euro. Phys. Lett. **83**, 67006 (2008); G. Wu, *et al*., J. Phys. Condens. Matter **21**, 142203 (2009); P. Cheng, *et al*., Euro. Phys. Lett.**85**, 67003(2009).

[21] Medvedev S. *et al*., Nat. Mater. **8**:630 (2009).

[22] Lei B. *et al*., Physical Review Letters **116**:077002 (2016).

[23] Sun H,Woodru_ DN. *et al*., Inorganic Chemistry **54**:1958-1964 (2015).

[24] Burrard-Lucas M. *et al*., Nature Materials 12:15 (2013).

[25] Qing-Yan W. *et al*., Chinese Physics Letters 037402 (2012).

[26] Wang Z. *et al*., Journal of Physics: Condensed Matter **29**:153001 (2017).

[27] Bohmer AE. *et al*., Phys. Rev. **B 87**:180505 (2013).

[28] Chareev D. *et al*.. CrystEngComm **15**:1989 (2013)

[29]Bohmer AE. *et al*., Phys. Rev. **B 94**:024526 (2016)

[30] B. Indrajit Sharma *et al*., Journal of Physics: Conference Series **765** (2016) 012004

[31] S. Kurth *et al*., Arnimallee **14**, D-14195(2003)

[32] P.Giannozzi *et al.,* Phys. Rev **B 89**,220502 (2014)

[33] S. Baroni *et al*., Rev. Mod. Phys. **73**,515 (2001)

[34] Hong-Yan Ln *et al.,* J Low Temp Phys **178**,355-366 (2015)

[35] H. Takahashi, *et al.,* Nature. **453** 376 (2008).

[36] M. Rotter, *et al.,* Phys. Rev. Lett. **101** (10): 107006 (2008).

[37] X.C. Wang, Sol. Sta. Comm**. 148** 538 (2008).

[38] A. Roque, *et al.,* RE&PQJ, **Vol.1**, No.15,(2017).

[39] A.S. Panfilov *et al.,* Fiz. Nizk. Temp**. 40**, 793–800 (2014)

[40] Setyawan, Wahyu, Curtarolo, Stefano, Computational Materials Science*.* **49** (2): 299–312 (2010).